16TH EUROPEAN CONFERENCE ON EARTHQUAKE ENGINEERING THESSALONIKI 18 - 21 JUNE 2018

THE ASSESSMENT AND REDUCTION OF SEISMIC RISK IN CABLE STRUCTURES

Alin RADU[1], Irina F. LAZAR[2], Anastasios SEXTOS[3]

ABSTRACT

Extreme earthquakes may produce significant financial damage and affect a large number of people, due to direct and indirect damage to structures and infrastructure. Transportation networks are essential parts of infrastructure, which can cause significant financial loss and downtime for large communities, as a result of extreme seismic events. An accurate risk assessment and high-performance risk reduction methods are essential tools for preparedness and resilience in case of catastrophic events.
This study focuses on the assessment and reduction of the seismic risk of cable-structures, such as cable-stayed bridges, which could be indispensable but vulnerable components of critical transportation networks. Cables are slender structures with low inherent damping, exposed to a wide range of day-to-day and extreme excitation. The seismic risk assessment is achieved through estimating seismic fragility for cables, which is a widely-used measure for structural reliability. The seismic risk reduction is achieved by implementing vibration-suppression devices, such as tuned-inerter-dampers (TID). Numerical examples are shown for realistic structures subjected to seismic loading.

Keywords: Risk assessment; Vibration control; Tuned-inerter damper; Cable structures; Earthquake ground motion

1. INTRODUCTION

Cable structures are widely used in civil engineering structures and infrastructure, and they may experience significant vibrations due to their low inherent damping (Rega, 2004 - Part I; Rega, 2004 - Part II). Vibration-suppression systems can be attached to cables to reduce unwanted vibrations, which could be of great benefit for cable-stayed bridges in reducing their response to strong seismic or wind loads. Studies on the efficiency of cables with attached viscous (Main and Jones 2001), or magneto-rheological dampers (Weber et al. 2005; Johnson et al. 2007) on cable-stayed bridges, have shown that the performance of these devices is restricted by the limitation that they need to be installed within 5% of the cable length. This disadvantage may be overcome by the use of the more complex and less practical tuned-mass dampers, which do not require connections with the deck and can be connected anywhere along the cable's length (Wu and Cai, 2006; Casciati and Ubertini, 2008). However, these are difficult to reach for maintenance purposes. More recently, the tuned-inerter damper (TID) was shown to overcome the limitations of the aforementioned devices, by reducing significantly the response of cable structures, while preserving the practical advantages of it being installed close to the anchorage point of the cable (Lazar et al. 2016). The TID is a passive control system proposed in (Lazar et al. 2014) and has a layout similar to that of passive tuned-mass dampers, where the mass element is replaced with an inerter (Smith 2002). The main feature of the inerter is that it can generate an apparent mass that is much higher than its physical mass (this is usually achieved via gearing). The

[1] Marie Curie Research Fellow, Department of Civil Engineering, University of Bristol, Bristol, UK, alin.radu@bristol.ac.uk
[2]Senior Research and Teaching Associate, Department of Mechanical Engineering, University of Bristol, Bristol, UK, irina.lazar@bristol.ac.uk
[3]Reader, Department of Civil Engineering, University of Bristol, Bristol, UK, a.sextos@bristol.ac.uk

force produced by an inerter is given by the product between its apparent mass, also known as inertance, and the relative acceleration across its terminals. Extensive research into the use of inerter-based vibration-control systems in civil engineering applications have been carried out recently, for example (Marian and Giaralis 2014; Lazar et al. 2016; Giaralis and Petrini 2017).
The goal of this paper is to analyze the reliability of TID-controlled cable structures under seismic loading. The TID is designed using the procedure proposed by Lazar et al. (2016), but the vibration-controlled cable structure is analyzed for a large range of simulated seismic ground-motion samples, rather than just for one single earthquake record. The cable-structure model will be regarded as an independent cable installed within a cable-stayed bridge. The performance of the bridge structure itself is beyond the scope of this study. The paper discusses the performance of the cable subjected to strong ground-motion and the limitations entailed by the assumptions of the model proposed. A numerical example is shown for a proxy model of a cable from the Evripos Bridge in Greece (Sextos et al. 2014) and simulated ground-motion samples are obtained using the specific barrier model (Halldorsson and Papageorgiou 2005).

2. STRUCTURAL SYSTEM

The structural system is assumed to be a cable fixed at both ends, that is, one end attached to the pylon of the bridge, and the other end attached to the deck of the bridge. The cable is in tension and it is assumed to have a TID installed near the deck end, connected to the deck of the bridge. Different excitations are applied at the two ends of the cable, each being determined by the response of the pylon and the deck to the earthquake input, respectively. The model used for the cable structure and the design of the TID are discussed in the following subsections.

2.1 Tuned-Inerter Damper

The TID is the selected device for the vibration-control of the cable. It is characterized by three parameters, the inertance-to-mass ratio between the inertance (the inerter's apparent mass which is significantly higher than its physical mass) and the total mass of the cable, the damping and the frequency ratios between the TID and the host structure (in this case, the cable). The damping ratio of the TID, relative to the cable is defined in (Lazar et al. 2016) as

$$\zeta = \zeta_0 \frac{\pi\mu}{\rho} \ , \tag{1}$$

where $\mu = b_d/m_c$ is the inertance-to-cable-mass ratio, and ρ is the TID-to-cable-natural-frequency ratio, and

$$\zeta_0 = \frac{c_d}{2\omega_d b_d} \tag{2}$$

is the TID damping ratio, where c_d is the damping coefficient of the TID, ω_d is the TID natural frequency, b_d is the inertance and m_c is the total mass of the cable. The TID design for the cable is performed following the procedure developed by Lazar IF et al. (2016). The method relies on the optimization of the TID's parameters installed on a simplified TID-controlled cable fixed at both ends and subjected to identical harmonic oscillation at both ends, such that the midspan displacement of the cable is minimized. The method provides design contour plots that allow the user to select the TID's parameters depending on the chosen TID location along the cable's length and the apparent mass of the inerter.

2.2 Cable Finite Element Model

A simple linear finite-element model as the one presented in (Lazar et al., 2016) is also used for the

cable problem analyzed in this study. The cable is divided in twenty, $N = 20$, axial elements, each of mass m_i, and stiffness k_i, $i = 1, \dots, N$, with the total mass of the cable $m_c = \sum_{i=1}^{N} m_i$. Since the TID must be connected between the cable and the bridge deck, its connection point is limited between 1% and 5% of the cable's total length, L. For simplicity, in this paper it will be considered that the TID is located at $5\%L$. Hence, for a model with $N = 20$ elements, all resulting cable segments will have equal lengths ($5\%L$). The installation of a TID results in the addition of one extra degree of freedom to the $N - 1$ degrees of freedom of the uncontrolled cable. The equation of the motion for the cable can be written as:

$$M\ddot{X}(t) + C\dot{X}(t) + KX(t) = -MA(t), \tag{3}$$

where $X(t)$ is the relative displacement vector and $A(t)$ is a matrix that shows the acceleration time history at each of the two supports of the cable. Note that the time histories at the two ends of the cable are different, since they capture the response of the bridge at the two ends. M, C and $K$are the mass, damping and stiffness square matrices of dimension $N - 1$ for the uncontrolled cable, and of dimension N for the TID-controlled cable. For the uncontrolled cable, the diagonal terms of the mass matrix are $M_{i,i} = (m_i + m_{i+1})/3$, for $i = 1, \dots, N-1$, while the off-diagonal terms are $M_{i,i+1} = M_{i+1,i} = m_{i+1}/6$ for $i = 1, \dots, N-2$. The mass matrix of the TID-controlled system has an additional line and column with the only non-zero term $M_{N,N} = b_d$, where b_d is the inertance of the TID. The diagonal terms of the stiffness matrix of the uncontrolled cable are $K_{i,i} = k_i + k_{i+1}$, for $i = 1, \dots, N-1$, while the off-diagonal terms are $K_{i,i+1} = K_{i+1,i} = k_{i+1}$ for $i = 1, \dots, N-2$. The stiffness matrix of the TID-controlled system has an additional line and column with the only non-zero terms $K_{N,N} = k_d$, $K_{1,N} = K_{N,1} = -k_d$, where k_d is the stiffness of the TID. Note that the term $K_{1,1}$ for the TID-controlled system becomes $K_{1,1} = k_1 + k_2 + k_d$. Since the cable is poorly damped, the damping matrix of the uncontrolled cable is assumed to be a null square matrix of dimension $N - 1$. However, when the TID is attached to the cable, the damping matrix is modified in a similar way as in the case of the stiffness matrix, described above.

For the numerical example in this paper, the cable considered for the study is one of the cables designed for the Evripos Bridge. It has a length of $42\ m$, a unit mass of $7.6\ kg/m$, it is subjected to an axial tension of $74\ kN$, and it forms an angle of approximately $82°$ with the deck.

3. SEISMIC RELIABILITY ANALYSIS

The seismic reliability of cable structure is analyzed by studying the performance of the uncontrolled and the TID-controlled cables subjected to a large range of seismic ground motions. Structural response is sensitive at the frequency content of the seismic ground motions, which is mainly governed by characteristics such the moment magnitude, m, source-to-site distance, r, and the local soil conditions. Due to the limited number of seismic ground motions available, a simple ground-motion simulation model is used to generate earthquake time histories, to which the cable structure is tested.

3.1 Ground-Motion Excitation

A simple model is used to characterize the seismic hazard, described by two main components: (1) the seismic activity matrix, which represents two-dimensional histograms giving the probability of occurrence $P_{m,r}$ of earthquakes with moment magnitudes m and site-to-source distances r, for a particular site, and (2) a ground-motion simulation model, which is used to simulate ground-motion time histories characterized by (m, r) and soil conditions.

The seismic activity matrix for a site in Los Angeles is shown in the left panel of Figure 1, and it is calculated using data from the USGS earthquake probability tool. The characterization of earthquakes by (m, r) is important because the frequency content of the motion is governed mainly by these two components. The right panel of Figure 1 shows the one-sided power spectral-density functions $g(v; m, r)$ for two types pf earthquakes characterized by three pairs of $(m, r) = \{(5.1, 10\ km)$,

$(6.5, 30\ km)$, $(7.3, 30\ km)\}$, for a soil characterized by the shear-wave velocity in the top $30\ m$ of soil $v_{s30} = 760\ m/s$. These functions are the result of the specific barrier model (SBM) (Halldorsson and Papageorgiou 2005), a seismological-source model that produces $g(v; m, r)$. Based on the frequency content provided by the SBM, ground motions are simulated using a simple model

$$A(t) = f(t)G(t),\ t \geq 0, \tag{4}$$

where $G(t)$ is a zero-mean, stationary, Gaussian process with second-moment properties characterized by the power spectral density $g(v; m, r)$, and $f(t) = \alpha t^{\beta} e^{-\gamma t}$ is an amplitude modulation function with scalar parameters α, β, γ, which are also functions of (m, r) and are provided by the SBM.

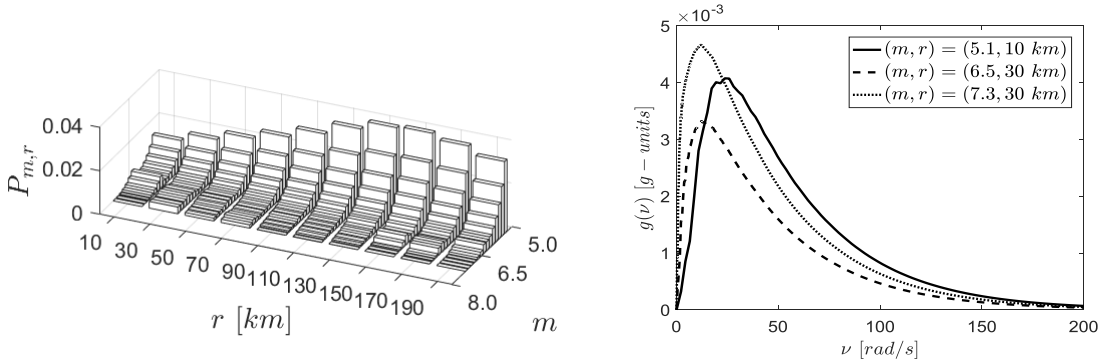

Figure 1. The seismic activity matrix for Los Angeles (left); the one-sided spectral density functions $g(v; m, r)$ for $(m, r) = (5.1, 10\ km)$, $(m, r) = (6.5, 30\ km)$, and $(m, r) = (7.3, 30\ km)$, respectively.

A number of $n = 1{,}000$ ground-motion samples $a_k(t), k = 1, \ldots, n$ of $A(t)$ have been simulated for each pair (m, r) of the seismic activity matrix, using the spectral-representation method.

Most of the cables in a cable-stayed bridge are connected to the deck and the pylons. Thus, the cable elements are not subjected directly to the ground motion itself, but to the response of the deck and the pylon, respectively. For the simulation of a more realistic load scenario at the two ends of the cable, the ground motion samples are initially passed through a linear single-degree-of-freedom filter meant to simulate the response of the bridge's deck and pylon.

The parameters of the filter have been chosen such that the responses of the deck and the pylon at the ends of the cable studied (i.e. from the Evripos Bridge in Greece) are consistent with the more complex analysis performed for the same cable in (Sextos et al., 2014). The response of the deck where the cable is connected is assumed to be characterized by a natural frequency of $0.25\pi\ rad/s$ and a damping ratio of 5%, while the response of the pylon at the cable-connection point is assumed to be characterized by the response of a single-degree-of-freedom linear oscillator with natural frequency $0.5\pi\ rad/s$ and damping ratio 10%.

3.2 Seismic Performance

One way of testing the seismic performance of TID-controlled cable versus the uncontrolled cable, is by comparing their maximum mid-span displacements. The left and middle panels of Figure 2 show the maximum mid-span displacements of the controlled and uncontrolled cables, respectively, as a function of (m, r) calculated from 1,000 simulations. The maximum responses are reduced, and the percentage difference in this reduction is shown in the right panel of Figure 2. It is noticed that in the case of the cable analysed, the TID reduces significantly, i.e. by 30% or more, the maximum response of the cables subjected to more probable earthquakes (see the left panel of Figure 1), i.e. earthquakes with magnitudes $m \leq 6$.

Although this method shows some idea on how the cables perform when subjected to different types of earthquakes, this measure is trivial and it is not reliable. A common measure of the reliability of structures subjected to seismic loads is the seismic fragility, which is the probability that the structural engineering demand parameter – in this case, midspan maximum absolute displacement – exceeds a

critical limit value for a given level of the seismic intensity measure. Since the structural response is sensitive to the frequency content of the input, mostly controlled by (m, r), seismic fragilities in this study are functions in the (m, r) space. We call the graphical representation of this probability a fragility surface and it is described by the following relation:

$$P_f(m,r) = \mathbb{P}\left(\max_{t\geq 0}|X_m(t)| > x_{cr} | (M,R) = (m,r)\right), \tag{5}$$

where $X_m(t)$ is the stochastic process representing the midspan displacement of the cable, at the middle node of the cable's finite-element model, as described in the previous section, and x_{cr} is a limit or critical maximum midspan displacement chosen by the designer.

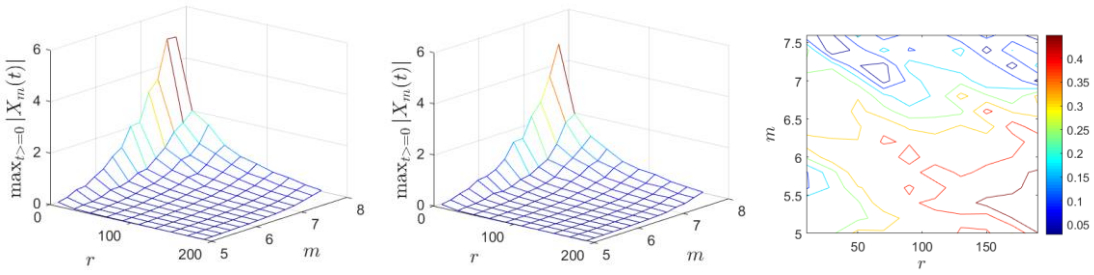

Figure 2. Maximum mid-span displacement of the uncontrolled (left) and TID-controlled (center) cables; percentage difference between maximum mid-span displacements (right).

The probability $P_f(m,r)$ can be calculated by Monte Carlo simulations using the n ground motions simulated for each value of (m,r) as

$$P_f(m,r) = \frac{1}{n}\sum_{k=1}^{n} \mathbb{1}\left(\max_{t\geq 0}\left|x_m^k(t)\right| > x_{cr} | (M,R) = (m,r)\right), \tag{6}$$

where $x_m^k(t)$ is the time response of the cable subjected to sample $a_k(t)$, at midspan. Figures 3 and 4 show the fragility surfaces for two different damage states of the cable, represented by a limit midspan displacement $x_{cr} = 0.1\ m$ and $x_{cr} = 0.5\ m$, respectively. The left and the right panels of these two figures show the fragility surfaces for the uncontrolled and the TID-controlled cable, respectively.

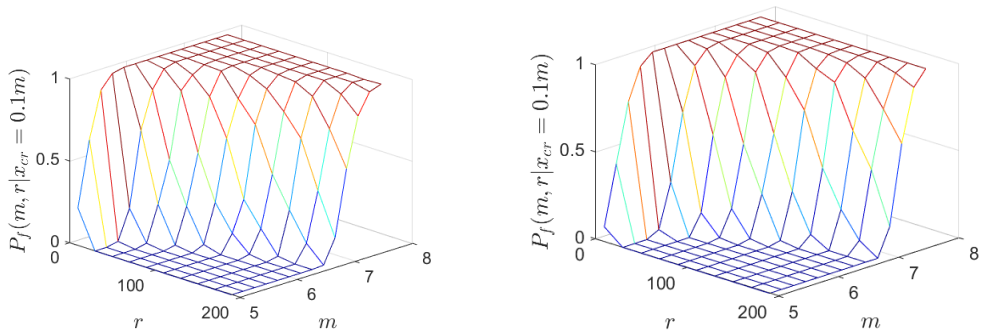

Figure 3. Fragility surface $P_f(m,r)$ for $x_{cr} = 0.1\ m$ for the uncontrolled cable (left) and TID-controlled cable (right).

The fragility surfaces provide some relevant information on the seismic performance of the TID connected to the cable as a function of (m,r) for specified levels of x_{cr}. However, this may be unpractical in design, since the seismic performance of a structure, as well as the design of the TID cannot be done according to each type of earthquake.

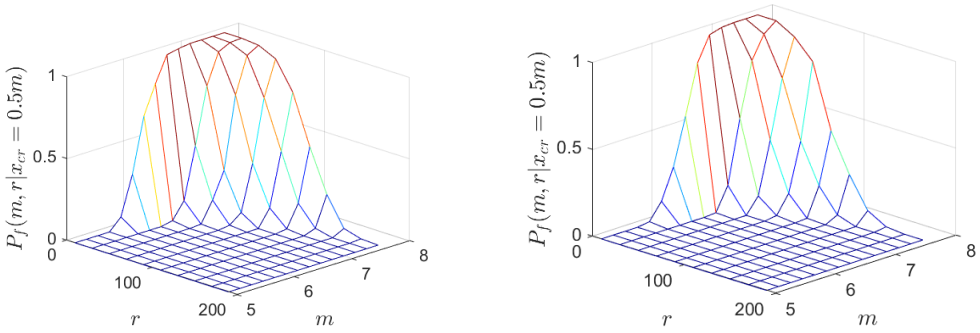

Figure 4. Fragility surface $P_f(m,r)$ for $x_{cr} = 0.5\,m$ for the uncontrolled cable (left) and TID-controlled cable (right).

Thus, the overall probability of exceedance of the uncontrolled and TID-controlled cables can be calculated by means of conditional probability:

$$F(x_{cr}) = \mathbb{P}\left(\max_{t\geq 0}|X_m(t)| > x_{cr}\right) = \mathbb{P}\left(\max_{t\geq 0}|X_m(t)| > x_{cr}|(M,R) = (m,r)\right)P_{m,r}, \tag{7}$$

where $\mathbb{P}\left(\max_{t\geq 0}|X_m(t)| > x_{cr}|(M,R) = (m,r)\right)$ is the fragility surface calculated in Equation 5, and $P_{m,r}$ is the probability of occurrence of an earthquake characterized by (m,r) and is provided by the seismic activity matrix shown in the left panel of Figure 1.

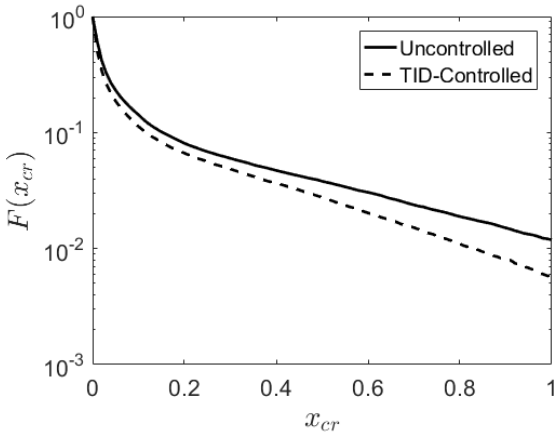

Figure 5. The overall tail probability $F(x_{cr})$ for the uncontrolled and the TID-controlled cables.

Figure 5 shows the overall probability of failure of the uncontrolled and the TID-controlled cables, calculated based on Equation 7. It can be noticed that the TID-controlled cable performs better than the uncontrolled cable for all levels of x_{cr}, even in the very extreme tails. It can be concluded that this current design for the TID-controlled cable reduces the seismic risk in the cable. However, it must be noticed that this conclusion applies to the cable structure only, and a more complex analysis is needed to establish whether the TID-controlled cables improve the reliability of cable-stayed bridges.

5. CONCLUSIONS

Cable are commonly used as load-bearing elements in civil engineering structures and infrastructures and the study of their performance under extreme loading is a key element when cables are used in the design of essential infrastructures, such as cable-stayed bridges. The reliability of cables subjected to seismic loads was studied in this paper and a vibration-control system was used to reduce the effects

of these powerful loads on the response of cables. The control of the vibration on the cables was achieved using a tuned-inerter damper (TID), and the performance of this device on the cable structures was assessed using a probabilistic seismic analysis. Simulated ground motions were used as the excitation for the finite-element model of the cable in order to calculate reliability metrics of the controlled and uncontrolled cable in terms of seismic fragility. The TID performed well in reducing the overall response of the cable structures under seismic loads, its performance however being affected by the frequency content of the motion. Further investigations should be performed on vibration-controlled systems as part of their host structures in order to establish the feasibility of installing such devices as a mean for achieving seismic-resilience of infrastructures.

6. ACKNOWLEDGMENTS

The work reported in this paper has been partly supported by the Marie Skłodowska-Curie Actions of the European Union's Horizon 2020 Program under the grant agreement 704679 - PARTNER. This support is gratefully acknowledged.

7. REFERENCES

Casciati F, Ubertini F (2008). Nonlinear vibration of shallow cables with semiactive tuned mass damper. *Nonlinear Dynamics*, 53(1–2): 89–106.

Giaralis A, Petrini F (2017). Optimum design of the tuned mass-damper-inerter for serviceability limit state performance in wind-excited tall buildings. *Procedia Engineering, 199*, pp. 1773–1778. doi:10.1016/j.proeng.2017.09.453.

Halldorsson B, Papageorgiou AS (2005). Calibration of the Specific Barrier Model to Earthquakes of Different Tectonic Regions. *Bulletin of the Seismological Society of America*, 95(4): 1276-1300.

Johnson EA, Baker GA, Spencer BF, Fujino Y (2007). Semiactive damping of stay cables. *ASCE Journal of Engineering Mechanics*, 133(1): 1–23.

Lazar IF, Neild SA, Wagg DJ (2014). Using an inerter based device for structural vibration suppression. *Earthq Engineering and Structural Dynamics*, 43(8): 1129-1147.

Lazar IF, Neild SA, Wagg DJ (2016). Vibration suppression of cables using tuned-inerter dampers. *Engineering Structures*, 122: 62-71.

Main JA, Jones NP (2001). Evaluation of viscous dampers for stay-cables vibration mitigation. *Journal of Bridge Engineering*, 6: 385–97.

Marian L, Giaralis A (2014). Optimal design of a novel tuned mass-damper–inerter (TMDI) passive vibration control configuration for stochastically support-excited structural systems. *Probabilistic Engineering Mechanics*, 38: 156 -164.

Rega G (2004). Nonlinear vibrations of suspended cables – Part I: Modeling and analysis. *ASME Journal of Applied Mechanics Reviews*, 57(6): 443–478.

Rega G (2004). Nonlinear vibrations of suspended cables – Part II: Deterministic phenomena. *ASME Journal of Applied Mechanics Reviews*, 57(6): 479–514.

Sextos A, Karakostasb C, Lekidis V, Papadopoulosa S (2014). Multiple support seismic excitation of the Evripos bridge based on free-field and on-structure recordings. *Structure and Infrastructure Engineering*, 11(11): 1510-1523.

Smith MC (2002). Synthesis of mechanical networks the inerter. *IEEE Transactions on Automatic Control*, 47: 1648-1662.

Weber F, Feltrin G, Motavalli M (2005). Passive damping of cables with MR dampers. *Journal of Materials and Structures*, 38(5): 568–577.

Wu WJ, Cai CS (2006). Cable vibration reduction with a hung-on TMD system. Part II: Parametric study. *Journal of Vibration Control*, 12(8): 881–99.